Stockholm University
Analytical Chemistry
Environmental Science and Analytical Chemistry

Practical aspects of LC-ESI-MS/MS method development for analysis of biological matrices

8 Credits

Undergraduate Internship Report

Analytical Chemistry

Thomas Ledbetter

2018

Collège des Sciences et Technologies pour l'Energie et l'Environnement – STEE
Campus de la Côte Basque

Licence Physique-Chimie

Ledbetter, Thomas

Stage effectué du 4/1 au 6/1 2019 au

Département de Science Environnemental et de Chimie Analytique
Université de Stockholm
Svante Arrhenius väg 16 C
114 18 Stockholm

Sous la direction scientifique de Mr. Leopold Ilag

8 Credits

Undergraduate Internship in Analytical Chemistry

Completed at

Department of Environmental Science and Analytical Chemistry

Stockholm University

Svante Arrhenius väg 16C

114 18 Stockholm

Supervisor: **Supervisor**

Leopold Ilag

Table of Contents

Abbreviations

5-HIAA	2-(5-Hydroxy-1-indol-3-yl) acetic acid
AC	Alternating Current
AQC	$C_{14}H_{11}N_3$ (6-aminoquinolyl-N-hydroxysuccinimidyl carbamate)
BMAA	β-methylamino-L-alanine)
BNF	Biological Nitrogen fixation
CE	Capillary Electrophoresis
CI	Chemical Ionization
DC	Direct Current
DEP	Diethyl Phalate $C_6H_4(COOC_2H_5)_2$
DESI	Desorption Electrospray Ionization
DHB	$(HO)_2C_6H_3CO_2H$
FS	Full Scan
ESI	Electro Spray Ionization
GOGAT	Glutamine oxoglutarate aminotransferase
HPLC	High Performance Liquid Chromatography
LLE	Liquid-Liquid Extraction
LLOD	Lower Limit of detection
LLOQ	Lower Limit of quantification
ULOQ	Upper Limit of quantification
MALDI	Matrix Assisted Laser Desorption Ionization
MRM	Multiple Reaction Monitoring
MS/MS	Multiple step ion selection with fragmentation
MSI	Mass Spectrometer Imaging; spatial distribution of analyte
NIST	National Institute of Standards and Technology (GC standard 70ev)
EI	Electron Ionization
P_i	PHO_3
PSI	Paper Spray Ionization
QC	Quality Control
SIM	Selected Ion Monitoring
SRM	Selected Reaction Monitoring
SPE	Solid Phase Extraction
TIR	Transition Ion Ratio
Tg	1 Teragram (= 10^{12} grams)
CAS#	Chemical Abstracts Service number

Abstract

The goal of this internship was to learn practical skills in chemical analysis through observation and involvement in two separate research projects. For the purpose of this report, concrete examples from each project have been used to discuss the instruments, theory and techniques implicated in each step of the analytical chain.

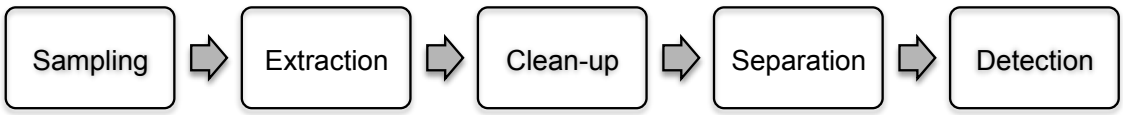

Figure 1: The classical analytical chain

For the “BNF project,” samples were extracted and derivatized before methods were developed for flavonoid analytes using LC separation and ESI-MS/MS detection with standards. Technical difficulties during the internship period halted sample analysis so results from the “5-HIAA project” were used to discuss gradient development, calibration, and quantification methods.

Combined experience from both projects demonstrated that careful method development can reduce the need for extraction and clean-up of complex matrices while increasing the accuracy and precision of results.

1. Introduction

1.1 BNF project

Global agriculture relies heavily on the cultivation of legumes and grains as they are widely consumed by humans and used to feed livestock. Legume cultivation is of particular interest for unlike grains, they are able to acquire N from Biological Nitrogen Fixation, (BNF). Nitrogen (N) assimilation plays a key role in fertilization as a required component of amino and nucleic acids responsible for plant growth and function. Global quantification of crops produced using BNF as a sole source of N was estimated by Herridge in 2008 at 50-70 Tg annually and has likely increased since. The most abundant natural source of N is earth’s atmosphere, making up roughly 78.1% of our air.

Nitrogen Fixation occurs when $N_{2(g)}$ is hydrogenated, a critical step in converting N into the oxidized state assimilated by plants. Currently, the Haber-Bosch process and BNF contribute equal amounts of NH_3 to sustain the world’s population [Hoffman 2014]. However, the former requires combustion of fossil fuels, releasing CO_2 and Nitrous Oxides that contribute to greenhouse effects and excess synthetic fertilizer can cause eutrophication [Ferguson 2010]. Interest in biofertilizers has increased with rising global agricultural demand,

and it has been suggested that increasing their use would be more sustainable and cost effective than current synthetic alternatives [Vance 2001].

Symbiosis between Legumes and soil bacteria from the α-proteobacteria family *Rhizobia* has been established as the most significant and reliable phenomena in quantifying BNF [Herridge 2008].

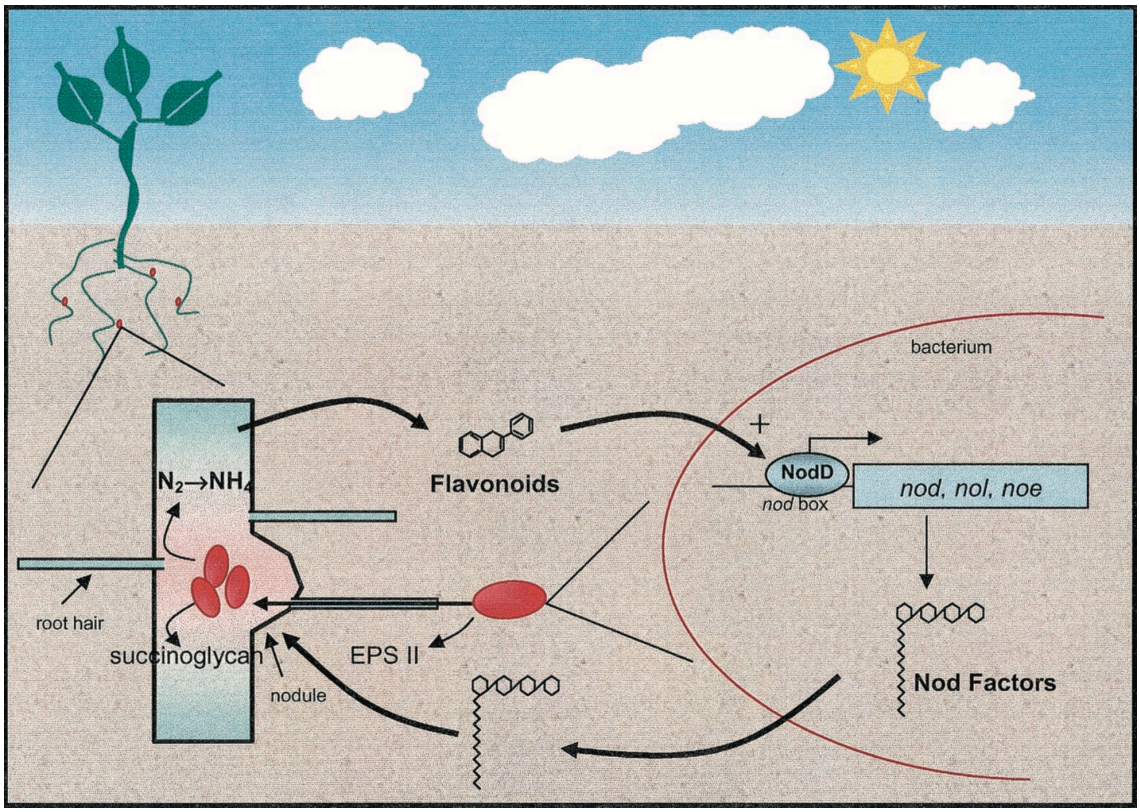

Figure 2: Symbiosis begins as root hairs of legumes secret flavonoids to which bacterium produce NOD factors in response, which in turn allow root hair curling and nodule organogenesis to occur within the plant root cell walls. The formation of the infection strain that allows bacterium to enter require *Rhizobia* to simultaneously produce exopolysaccharides. The exopolysaccharides EPS II and succinoglycan pictured in Figure 1 are specific to *Sinorhizobium meliloti* during symbiosis with *Medicago truncatula* [Gonzalez and Marketon 2003]

Once symbiosis is established, metabolite exchange and regulation occur, producing amino acids such as glutamine and glutamate [Gibson 2008].

BNF is a complex enzymatic reaction involving nitrogenase occurs under microaerobic conditions due to Leghemoglobin regulation of O_2 levels within the formed nodules [Denison 1992, Gemperline 2014].

$$N_{2(g)} + 16MgATP + 8e^- 8H^+ \rightarrow 2NH_3 + H_{2(g)} + 16MgADP + P_i$$

[Peters and Szilagyi 2006]

The BNF project aimed to determine the efficiency of BNF within the symbiotic system of α-proteobacteria *Rhizobium leguminosarum bv. vicae* and crop plant *Pisum sativum L*.

1.1.2 5-HIAA project

2-(5-Hydroxy-1-indol-3-yl) acetic acid (5-HIAA) is a metabolite of the endogenous neurotransmitter 5-hydroxytryptamine (serotonin) and its concentration in urine is used to monitor carcinoid tumors [Lionetto 2008]. The aim of the 5-HIAA project to identify and quantify this biomarker within urine samples.

1.2 Instrumental analysis: The LC-ESI-MS/MS system

1.2.1 HPLC

An atom's potential to attract shared electron pairs towards it nucleolus when covalently bonded with other atoms is quantified with the Pauling scale of electronegativity. Every compound has a net dipol moment and liquid chromatography exploits differences in polarity to separate analytes from other compounds present in the sample matrix.

A binary mobile phase is used to control the elution time of the analyte. In the beginning of the run, the mobile phase consists primarily of a solvent "A" that has different chemical properties than the analyte but similar chemical properties to extraneous compounds. During this time the analyte remains in the column thanks to attractive Van der Waals interaction with the stationary phase lining its perimeter as Solvant A elutes extraneous compounds. Gradual dimishment of solvent A and an increase in the solvent "B" (that has imilar chemical properties to that of the analyte) causes the analyte to elute as its interaction with solvent "B" overcomes its interaction with the stationary phase.

In both projects, reverse-phase chromatography was used as the stationary phase and analytes were compounds of low polarity and their interaction was hydrophobic. Solvent A was very polar and solvant B was very non-polar. Column dimensions, particle size, stationary phase thickness and type of matrix were taken into consideration when adjusting pressure and temperature settings for each analyte method.

1.2.2 Electro-Spray Ionization

After separation, compounds are volatilized and ionized using electrospray ionization. This "soft" technique creates ions without fragmentation of the analyte.

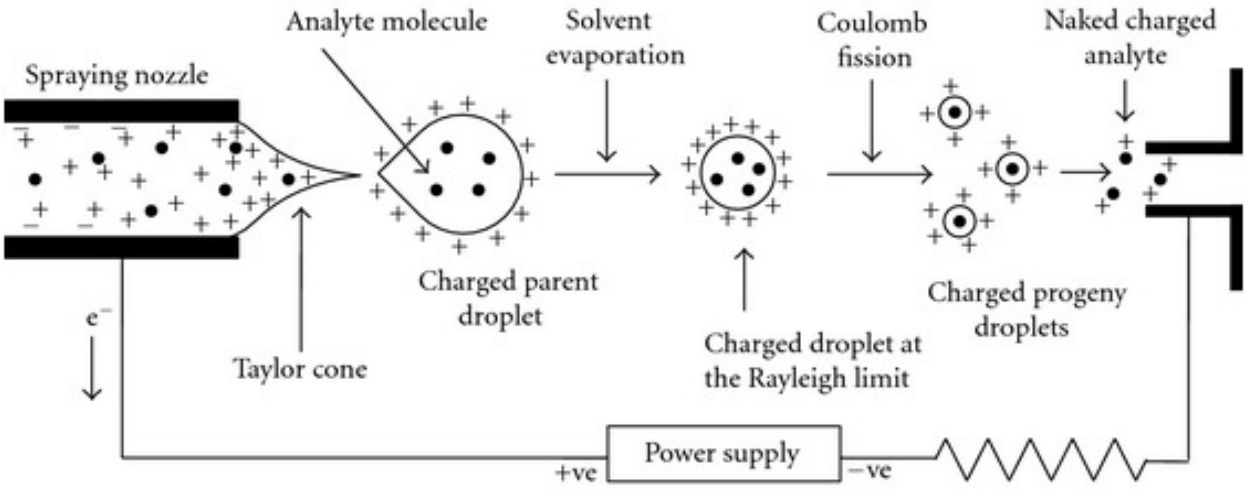

Figure 3: Banerjee and Mazdumar 2012

1.2.3 Triple Quadropole Mass Spectrometer

After ionization, charged analytes pass through a triple quadropole system that accelerates all ions present within a sample to a detector during a full scan (FS). The two pairs of rods in the quadropole use two oscillating (AC) electrical potentials to trap ions while a third static (DC) potential accelerates them through each quadropole chamber created by the rods.

The Quadropole system can also filter and fragment ions so that one (SRM) or several (MRM) parent to product ion transitions can be selected for detection. The first Quadropole selects parent ions as voltage between rods is adjusted so ions of desired m/z maintain a straight trajectory into the next Quadropole with extraneous ions being deviated. Selected parent ions are accelerated into a sealed chamber containing inert gas and the second Quadropole. Within this collision cell, parent ions are forced into contact with inert gas molecules and collision energy is adjusted to optimize fragmentation, creating product ions. Product ions of desired m/z are selected and filtered by the third Quadropole before detection.

2. Materials and Methods

2.1 Chemicals

Water from both projects was purified with a Millipore water purification system (Milli-Q IQ 7000) and had a resistance > 18 MΩ / cm.

2.1.1 BNF project

3-indole acetic acid, Indole-3-butyric Acid, Naringenin, Hesperitin, and L-Asperigine were purchased from Sigma-Aldrich (Saint Louis, MO, USA).

2.1.2 5-HIAA project

Acetonitrile was purchased from Rathburn (Walkerburn, Scotland). Formic acid (98-100%), 5-hydroxyindole acetic acid (>98 %) was purchased from Sigma-

Aldrich (Saint Louis, MO, USA). 5-hydroxyindole-4,6,7-d3-3-acetic-d2 (100 µg/mL in methanol) was purchased from Cerilliant (Texas, USA).

2.2 Analytes

Table 1: Names and CAS numbers of target analytes, precursor ion, collision energy and product ion used for Lider project using SRM-MS/MS analysis.

	CAS No.	Molecular Mass [Da]	Precursor Ion [m/z]	Product Ion [m/z]	Collision Energy [eV]	Retention Time [min]
3-Indoleacetic Acid[1]	87-51-4	175.18	176			
Indole-3-butyric Acid[2]	133-32-4	205.25	205			
(±)-Naringenin[3]	67604-48-2	272.25	271	151	15	3.73
(±)-Hesperitin[4]	69097-99-0	302.28	301	163, 242, 286	30	5.17
L-Asparagine[4]	85-68-7	132.12				
L-Glutamic acid[5]	56-86-0	147.13				
L-Glutamine	56-85-9	146.146				
L-BMAA[6]	15920-93-1	118.13				

Naringenin

5, 7-Dihydroxy-2-(4-hydroxyphenyl)chroman-4-one

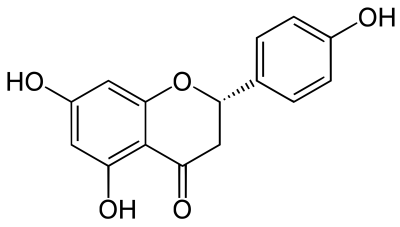

Hesperitine

(S)-2,3-Dihydro-5,7-dihydroxy-2-(3-hydroxy-4-methoxyphenyl)-4H-1-benzopyran-4-one

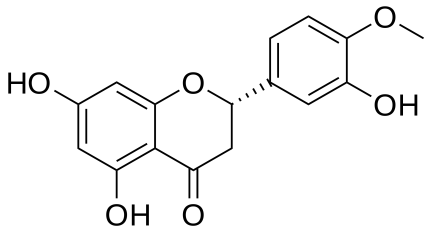

Asperigine

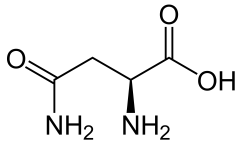

L-Glutamic acid

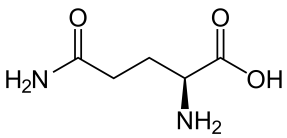

BMAA

(2*S*)-2-Amino-3-(methylamino)propanoic acid

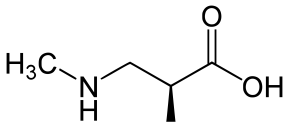

IBA

4-(1*H*-Indol-3-yl)butanoic acid

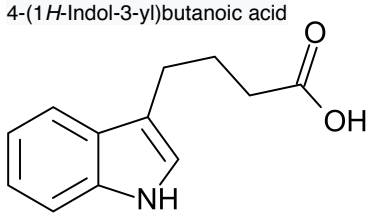

IAA

(2-(1*H*-indol-3-yl) acetic acid

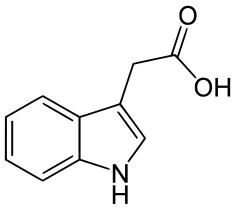

Table 2: Names and CAS numbers of target analytes, precursor ion, collision energy and product ion used for 5-HIAA project using SRM-MS/MS analysis.

	CAS No.	**Molecular Mass [Da]**	**Precursor Ion [m/z]**	**Product Ion [m/z]**	**Collision Energy [eV]**	**Retention Time [min]**
5-HIAA[1]	54-16-0	191.1	192.1	146.1, 118.1	13	4.49
D5-5-HIAA[2]	1219802-93-3	196.21	197.69	150.29	16	4.49

Suppliers were: 7 Sigma-Aldrich, Saint Louis, MO USA;8 Cerriliant (Texas, USA)

5-HIAA

2-(5-Hydroxy-1 H-indol-3-yl) acetic acid

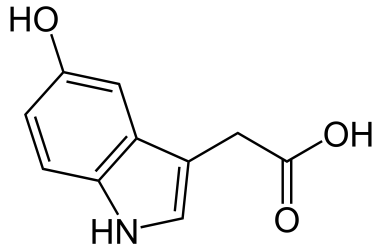

2.3 Sampling and preparation

2.3.1 BNF project

Seeds from crop plant *Pisum sativum L*. were treated with a biofertilizer containing NOD factors, produced by α -proteobacteria *Rhizobium leguminosarum bv. Vicae* which had previously been induced by the flavonoid

naringenine *in vitro*. Plants were grown in a greenhouse in Poland and root nodules were collected after 2, 3, and 6 weeks of growth. Tissue extraction was done following protocol outlined by Gemperline et al [2014] with some modifications (Appendix 1).

Free BMAA, Glutamine, Glutamate and Asperigine within samples treated with the Waters AccQ•Tag^{TM} Ultra Derivatization Kit (Appendix 3). The established MRM method was used for final analysis [Spáčil 2010].

All standards were in powder and were prepared for method development and internal standard for quantification.

2.3.2 5-HIAA project

Human urine samples were obtained from two volunteers in Stockholm, Sweden. Both individuals had no known medical issues or outstanding diet irregularities. Samples were diluted with water and spiked with liquid internal standard (IS) (a five-deuterated form of the analyte, D_5-HIAA) to have 1 ppm in each sample. Samples were vortexed and filtered using 0.45 µm PVDF filters (Pall Corporation, USA) before injection.

The calibration standard was in powder form and a stock solution of 100 ppm was prepared. Three sets of dilutions per calibration standard solution were done during the development of the calibration curve. The final calibration curve had six concentrations and a range of 5-750 ppb.

2.5 Instrumentation

2.5.1 BNF project

For the analysis of metabolites relevant to the Lider project, the LC-ESI-MS/MS system used was comprised of a C18 HPLC column (Agilent, 100× 3.0 mm, 3.5 µm particles) an Accela pump, a degasser and an Acella auto-sampler coupled with a TSQ Vantage triple quadrupole mass spectrometer (Thermo Fischer Scientific, San Jose, USA).

2.5.2 5-HIAA project

For the analysis of 5-HIAA, an LC-ESI-MS/MS system was used consisting of an Acquity UPLC Binary solvant manager pump, a degasser and an Acquity Sample Manager coupled with a Xevo® TQ-S Mass Spectrometer (Waters Corporation, Milford, USA). For chromatographic separation, an X-terra C18 column (150x2.1mm i.d. 3,5 µm, Waters, Milford, USA) coupled with an X-terra C18 guard column (30x3mm i.d. 2.5 µm, Waters, Milford, USA).

3. Results

3.1 BNF project

A method for Flavonoids naringenin and hesperitin was successfully developed, but due to technical difficulties and time constraits method development and sample results for the remaing analytes is ongoing.

Table 3: Gradient for Flavonoids.
Solvant C: H_2O + 0.1% formic acid (1mM)
Solvant D: Acetonitrile + 0.1% formic acid (1mM)

Time (min)	C (%)	D (%)	Flow (mL/min)
0	77	23	0.3
3.5	40	60	0.3
6	35	65	0.3
7	77	23	0.3
11	77	23	0.3

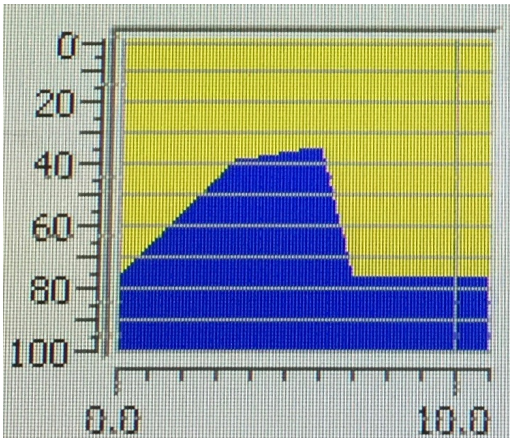

Table 4: MS tune settings for the Flavonoids

Spray Voltage	4000 V
Vaporizer Temperature	200 ºC
Sheath Gas Pressure	20 B
Ion Sweep Gas pressure	0,0 B
Aux Gas Pressure	10 B
Capillary Temperature	350 ºC
S lens RF amplitude	75
Declustering Voltage	0 V

3.2 5-HIAA project

A method and calibration curve were successfully developed for 5-HIAA. Bodén and Österlind [2019] found 212.1 and 261.1 ppb of 5-HIAA with relative standard deviation of 2.6 and 1.1 percent respectively in two urine samples from healthy subjects. Results were relatively accurate when compared to the 290 ppb found in healthy patients by Grouzmann et al. in 2018.

Table 5: Gradient for 5-HIAA project.
Solvant A: H_2O + 0.1% formic acid (1mM)
Solvant B: Acetonitrile + 0.1% formic acid (1mM)

Time (min)	Flow (ml/min)	A (%)	B (%)
0	0.2	90	10
5	0.2	10	90
7	0.2	10	90
7.1	0.2	90	10
10	0.2	90	10

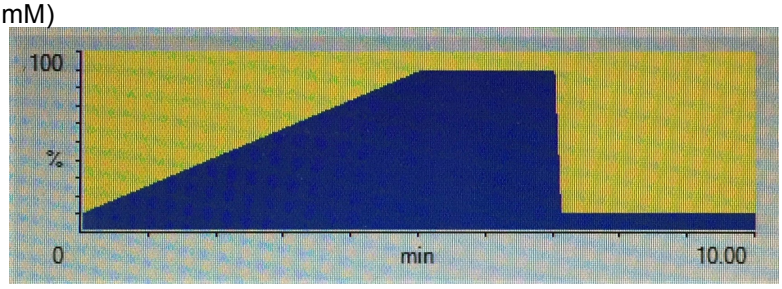

Figure 5: Final Gradient for 5-HIAA project

Figure 6: Final calibration curve for 5-HIAA project

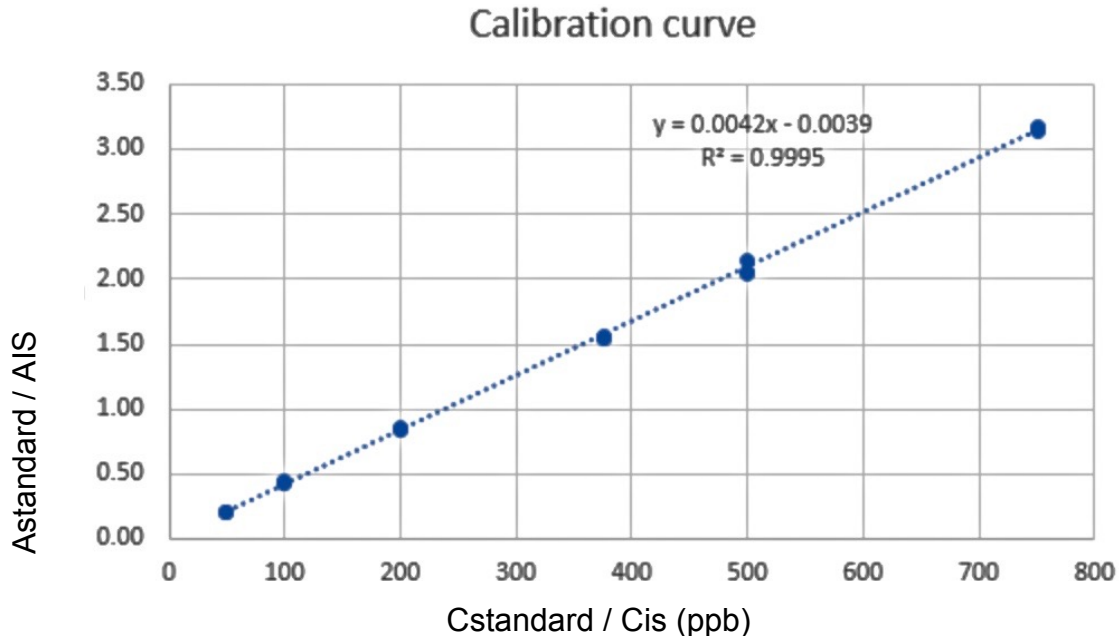

4. Discussion

4.1 Method development

4.1.2 MS tuning

Figure 7: The far left tube from the autosampler-LC (Acella) has been disconnected from the ESI-MS (Thermo-Fischer Scientific) and the MS inlet is connected to a tube leading the syringe loaded with 300 µL of prepared standard.

MS tuning ensures ionization and MS settings are adjusted to produce the highest intensity signal for a given ion's mass. After the syringe and tubes are

in place (Figure 1), “MS-only” and the type of scan (FS, SIM, SRM, or MRM) are selected using a procedural software program. As the standard is ionized and received by the detector, MS tune settings are adjusted in real time while peak intensity is monitored (Figure 2).

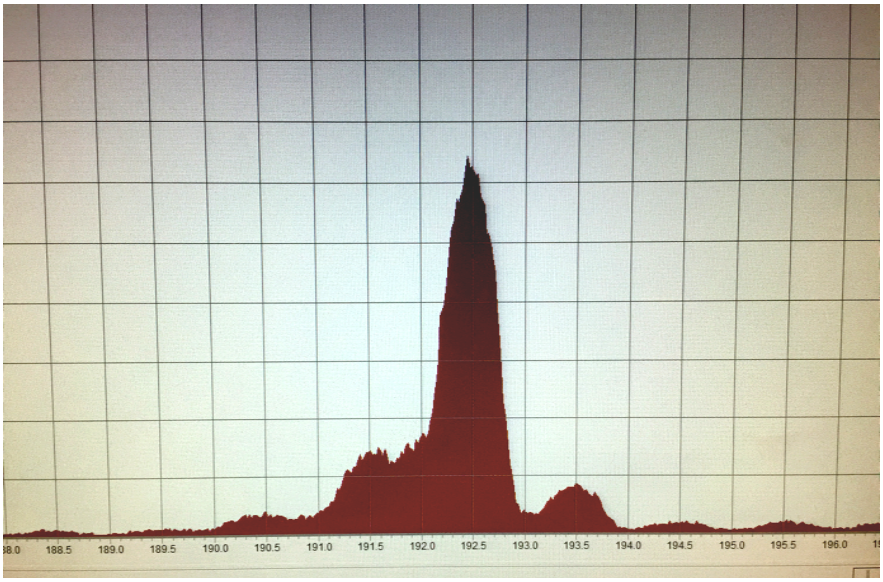

Figure 8: A SIM scan in positive ionization mode for the parent ion of analyte 5-HIAA (192.1 da). The gridded backdrop facilitates estimation of s/n ratio as parameters are optimized for maximal intensity.

The sensitivity of MS instrumentation detects very low concentrations of compounds within a matrix and precise detection limits specific to instruments and compounds are determined experimentally. The mean intensity of signals appearing in a blank sample containing only matrix is referred to as noise. If the signal to noise (S/N) ratio for a specific peak is 3:1 or higher, the peak can be used to identify a compound, and at 10:1 it can be used for quantification.

The smallest amount of the analyte that can be detected by the MS is referred to as the (LOD) and is found by adjusting MS tuning parameters and using the standard deviation of the blank. A lower detection limit reduces the amount of standard needed to run gradient development, calibration and QC sequences, thus increasing precision and accuracy. Additionally, excess concentration of analyte can the saturate the column and cause fronting in chromatograms as the excess analyte co-elutes early with non-target compounds.

4.1.3 Liquid Chromatography (5-HIAA Project)

The first step in developing a separation method was to adjust the flow rate to the was adjusted column used for the 5-HIAA project had different dimensions than the one used in the referenced literature, so the:

$\Delta P = \frac{\eta F L}{K \pi r^2 d_p^2}$

P = pressure (Pa) r = column radius (m)

d_p = particle diameter size (μm) η = dynamic viscosity (Pa · s)

F = flow rate (ml/min) L = length of column (m)

For column 1 (reference column) and column 2 (project column), we have:

$P_1 = \frac{\eta F_1 L_1}{K \pi r_1^2 d_p^2}$ $P_2 = \frac{\eta F_2 L_2}{K \pi r_2^2 d_p^2}$

If the solvents pressure from the literature are maintained, ($P_1 = P_2$, η and K constant) the following is obtained:

$$F_2 = F_1 \cdot \frac{L_1}{L_2} \cdot \left(\frac{d_{p2}}{d_{p1}}\right)^2 \cdot \left(\frac{d_2}{d_1}\right)^2$$

Thus a new flow rate F_2 was determined using the new project and reference column dimensions, L, diameter (d) and d_p.

Next, a solution of 1 ppm of IS and 40 ppm 5-HIAA calibration standard was run with several binary solvent gradients to produce narrow, high intensity peaks.

Figure 9: Chromatograms for Gradient 5 (RT=5.6 min) and Gradient 4 (RT=6.49 min). Both peaks had an intensity of e8 (10^8)

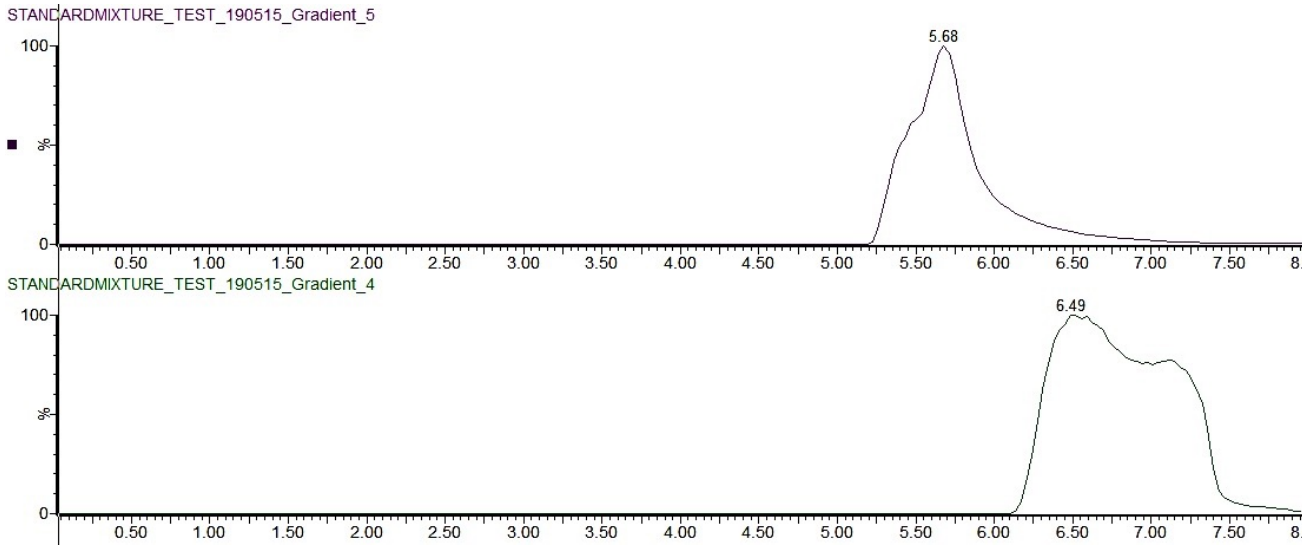

Table 6: Gradient development for 5-HIAA

Gradient 4					Gradient 5			
Time (min)	**Flow (ml/min)**	**A %**	**B %**		**Time (min)**	**Flow (ml/min)**	**A %**	**B %**
0	0.1	90	10		0	0.1	50	50
2	0.1	5	95		5	0.1	10	90
5	0.1	5	95		10	0.1	10	90
7	0.1	90	10		10.01	0.1	50	50
8	0.1	90	10		11	0.1	50	50

A sharp linear increase of solvent B in gradient 4 resulted in a broad peak, suggesting a co-elution of the analyte with several other organic compounds.

Though this continued in gradient 5, a slightly linear increase in solvent B from 0-5 minutes may account for some improvement. The increased tailing (continued slow elution after the peak maximum) suggests the analyte did not elute completely and immediately.

Final Gradient

Time (min)	Flow (ml/min)	A (%)	B (%)
0	0.2	90	10
5	0.2	10	90
7	0.2	10	90
7.1	0.2	90	10
10	0.2	90	10

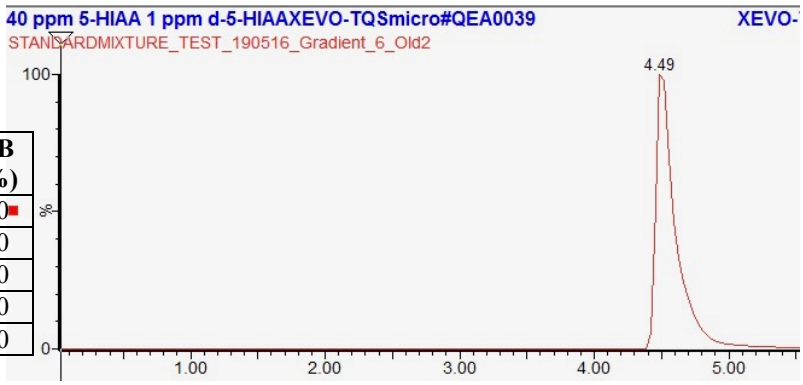

Figure 10: Final gradient Chromatogram. Intensity was 3.73 e8

For the final gradient, flow rate was increased to 0.2 and dwell time (data points taken per second) was changed from 0.5 to 0.7 minutes to reduce retention time and tailing, respectively. The gradual linear increase from 0-5 minutes eluted matrix compounds of higher to mid polarity until solvent B was in majority. A first isocratic (constant ratio of solvent) interval with a high percentage of solvent A from 5-7 minutes helped the analyte elute completely after being bound to stationary phase alkyl groups. The second isocratic interval returned the column to the equilibrium that begins the next run.

4.2.4 Calibration (5-HIAA Project)

The calibration curve is a sequence of at least six vials increasing in concentration of the standard over an interval. Ideally, it is run with every batch of samples or standards and is used to quantify the analyte using the following equations:

Given A = peak area after integration, C = concentration in ppm and $f_x = A_x/C_x$, $f_{IS} = A_{IS}/C_{IS}$ reponse factors of analyte standard (x), and the internal standard, respectively;

Relative response factor =

$$F_x = \frac{fx}{fis} = \frac{Ax}{Ais} \bullet \frac{Cis}{Cx} \quad (1)$$

By isolating the Ax/AIS quotient, we obtain:

$$\frac{Ax}{Ais} = F_x \bullet \frac{Cx}{Cis}$$

C_{IS} = constant (1 ppm for the 5-HIAA project)

Using the Cx/CIS as independent variables and Ax/AIS as dependent variables, we obtain F_x and a y-intercept value by linear regression. Theoretically, when analyte concentration is 0 ppm, y-intercept = 0. Experimentally, regression yields a non-zero y-intercept value due to errors in concentration of prepared standards and response data. The equation becomes:

$$\frac{Ax}{Ais} = F_x \bullet \frac{Cx}{Cis} + \text{y int.}$$

By injecting the F_x and y-intercept values obtained by regression of the calibration curve into (1), the concentration in a sample is:

$$F_x = \left(\frac{Asample}{Ais} - y\,\text{int}\right) \bullet \frac{Cis}{Csample} \rightarrow C_{sample} = \left(\frac{Asample}{Ais} - y\,\text{int}\right) \bullet \frac{Cis}{Fx}$$

$$\frac{Csample}{Cis} = \left(\frac{Asample}{Ais} - y\,\text{int.}\right) \bullet \frac{1}{Fx} \quad (2)$$

To quantify using equation (2), several conditions must first be met:

1) R^2 is a value close to 1 by a factor of < 10^{-3}

2) Integration values from sample analyte responses are within the interval of those from the calibration curve

3) Quality control (QC) sequences must verify the curve's accuracy.

In the 5-HIAA project, the second condition was verified during preliminary screening. One urine sample were spiked with 2.5 ppm of standard and the quantifier ion transition 192>146.1 was monitored. After integration, the following data was used to calculate the difference in spiked response vs. sample response:

	Retention time (min)	Area
"Ice man" urine sample	4.52	154199.31
Spiked Iceman urine sample	4.52	3996359.5

A_{spiked} - A = 3842160.19

$(A_{spiked} - A) / A = 24.91$

The response from the spiked Iceman sample was approximately 25 times that of the unspiked sample. An additional run found that responses from the ASD sample spiked with 0.5 ppm of standard were 30 times that of the unspiked sample. It was estimated that concentrations of [0.01- 0.1] ppm could be expected from samples, and as a result the LLOQ was changed to 0.01 ppm.

All calibration curves were run with an additional QC sequence. Injection started from the LLOQ up to the ULOQ and solvent blanks were run between every injection to avoid and estimate carryover.

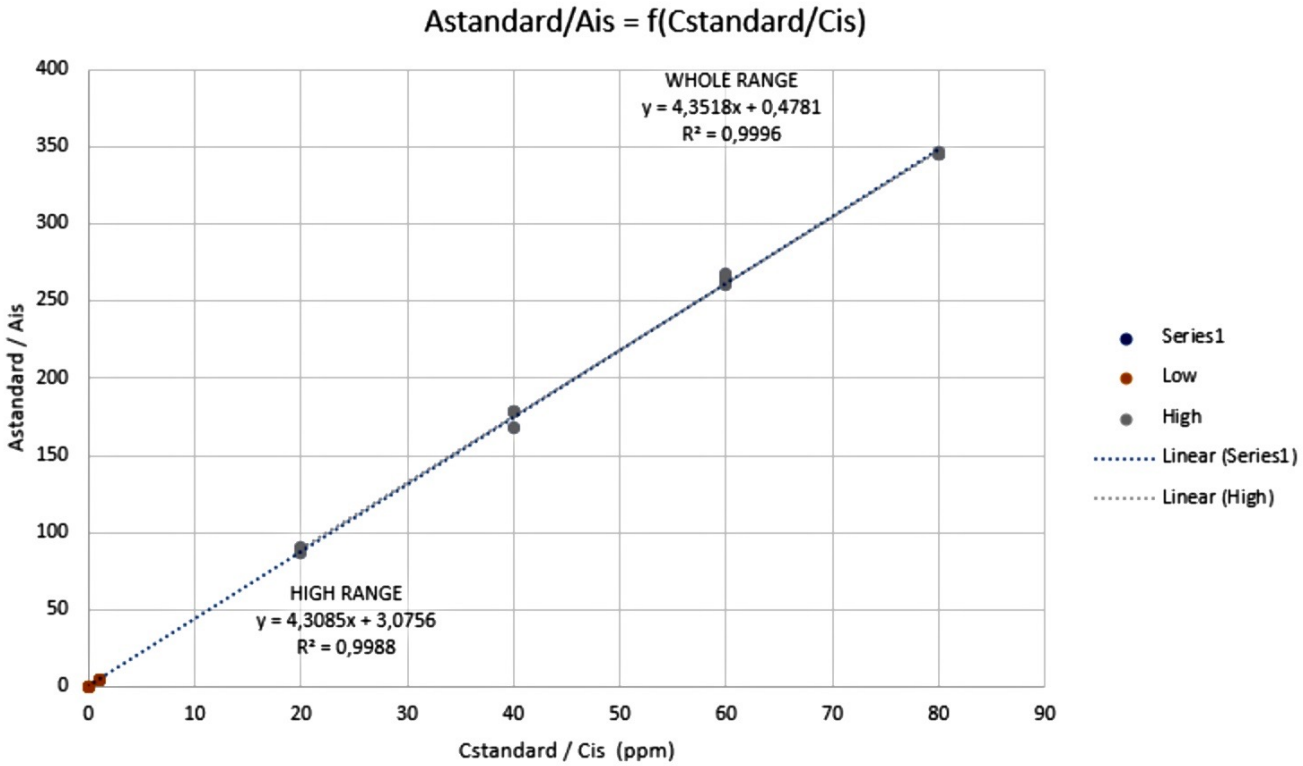

Figure 11: Pictured is the "first batch" standard calibration curve, with Cis = 1ppm. "Whole Range" refers to 0-80 ppm.

Table 8: Data form the first QC sequence. For each concentration, 3 injections were done to have a statistically relevant sample size. Some outlier values were disregarded for estimation purposes.

		5-HIAA			D5-5-HIAA		
	C (ppm)	**Rt**	**Area**	**Rt**	**Area (AIS)**	**A/AIS**
LLOQ1	0.01	4.45	38293.39	4.45	937943.6	0.040827
LLOQ2	0.01	4.45	36055.77	4.45	814865.31	0.044248
LLOQ3	0.01	4.45	30964.04	4.45	771870.5	0.040116
3xLLOQ1	0.03	4.45	121868.96	4.45	874656.25	0.139334

3xLLOQ2	0.03		-	-		-	-	
3xLLOQ3	0.03		4.45	95401.08		4.45	730383.19	0.130618
MLOQ1	40		4.45	57709112		4.45	319187.44	180.800072
MLOQ2	40		4.45	48499756		4.42	282886.06	171.446256
MLOQ3	40		4.45	47752344		4.42	272059.69	175.521570
ULOQ1	67		4.45	74506192		4.42	271277.22	274.649644
ULOQ2	67		4.45	66557384		4.45	234729.59	283.549185
ULOQ3	67		-	-		-	-	

The first calibration curve ranged from [0.01-80] ppm. After regression, F_x and y-intercept values were inserted into equation (2) along with A/AIS values from the QC sequence (Table 1) to calculate concentrations for each point on the calibration curve. Comparison of these results with the QC standard concentrations produced inaccurate results, so the curve was divided:

Low range : 0.01-1 ppm

- $y = 4.47266x + 0.008350541$ with $R^2 = 0.99840204$

High range : 20-80 ppm

- $y = 4.308539967x + 3.075546667$ with $R^2 = 0.998806874$

The y-intercept value from the high range equation cannot be used for quantification without obtaining negative concentration values.

Thus F_x and y-intercept values from the low range equation, A/AIS data from Table 5 and equation (2) were used for quantification “C Calc.”

Table 9: Evaluation of quantification capacity for the low range calibration curve. “C calc” values were found to have significant relative error, especially for the LLOQ. Some outlier values were disregarded for estimation purposes.

	C C (ppm)	C calc (ppm)	Rel error %	Mean (Rel error)	STDdev	RSD %
LLOQ1	0.01	0.00725	-27.50024	-25.4812	0.0005	6.63
LLOQ2	0.01	0.00801	-19.85261			
LLOQ3	0.01	0.00709	-29.09072			
3xLLOQ1	0.03	0.02927	-2.420201	-5.66794	0.0014	4.87
3xLLOQ2	0.03	0.02733	-			
3xLLOQ3	0.03	41.37596	-8.915683			
MLOQ1	40	39.21951	3.439904	-2.47567	1.0812	2.69
MLOQ2	40	40.15904	-1.951219			
MLOQ3	40	63.01225	0.397610			
ULOQ1	67	65.06397	-5.951862	-4.42073	1.4508	2.27
ULOQ2	67	0.00725	-2.889593			
ULOQ3	67	-	-			

A second batch was run with a calibration sequence across a range of (5-750 ppb) along with a matching range QC sequence.

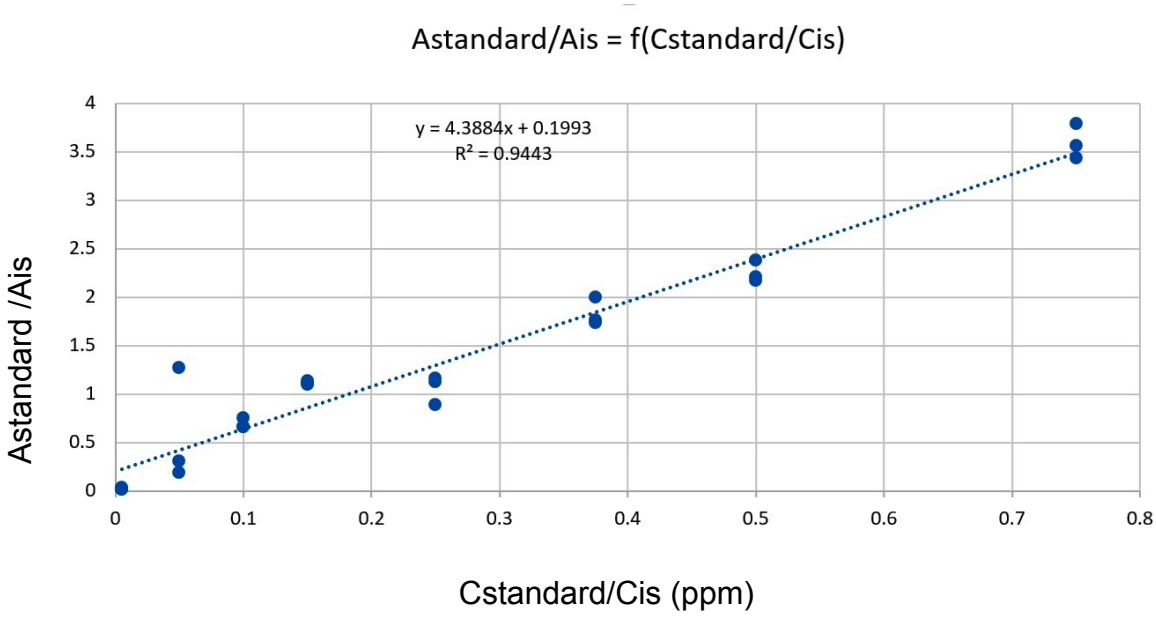

Figure 12: Scatterplot with linear regression for the second standard sequence using a (5-750 ppb) calibration curve with 3 injections per Cstandard. concentration value are relatively far from the trendline and R^2 is not close enough to 1 to be used for quantification. Additionally, y-intercept > A/AIS values for 5 ppb (mean = 0.021549).

Because the 5-750 ppb calibration curve was deemed unreliable for quantification, a new curve was created from the QC sample data in Table 3, yielding the following equation across a range of 5-500 ppb:

- $y = 4.679989926x - 0.003625811$ with $R^2 = 0.999719764$

Table 10: After quantification, significant relative error persisted for LLOQ

	C (ppm)	AA/AIS	C calc 2 (ppm)	Mean	Rel error (%)	RSD(CV) %
LLOQ1	0.005	0.02048	-0.00903	<1	<1	<1
LLOQ2	0.005	0.02003	-0.00913			
LLOQ3	0.005	0.020292	-0.00908			
LLOQ4	0.005	0.020554	-0.00902			
LLOQ5	0.005	0.02121	-0.00888			
3xLLOQ1	0.015	0.069348	0.021724	0.021867	45.8	0.780819
3xLLOQ2	0.015	0.070168	0.021896			
3xLLOQ3	0.015	0.070977	0.022066			
3xLLOQ4	0.015	0.069376	0.02173			
3xLLOQ5	0.015	0.070284	0.02192			
MLOQ1	0.25	1.1323	0.244514	0.249943	-0.0001	1.940959
MLOQ2	0.25	1.161634	0.250662			
MLOQ3	0.25	1.177981	0.254088			
MLOQ4	0.25	1.163823	0.251121			
MLOQ5	0.25	1.155275	0.249329			
ULOQ1	0.5	2.299085	0.489066	0.497714	-0.5	1.143178
ULOQ2	0.5	2.353367	0.500444			
ULOQ3	0.5	2.325266	0.494554			
ULOQ4	0.5	2.347476	0.499209			
ULOQ5	0.5	2.376519	0.505296			

To compensate for these errors, low concentrations of the third batch were prepared by diluting the stock solution and using a two-step dilution process to reduce pipette errors.

4. Conclusions

Several important factors from each project warranting discussion were not included due to time constraints. The 5-HIAA project evaluated the matrix effect in urine, carryover and ion suppression. Quantification of results from the BNF projects is ongoing and may be linked to BMAA research (Appendix 2).

To conclude, development of separation and detection methods was the central aspect of both projects. The quadropole system filtered non-target signals from two complex biological matrices, precisely monitoring desired ion transitions and allowing for quantification of 5-HIAA with an LOQ of 75.8 ng/ml and very little sample preparation. The theory and reasoning behind method development can be adapted to other research projects.

5. Perspectives

5.1 Research perspectives

Prior to handling I was given a selection of published scientific articles relevant to the BNF and 5-HIAA projects and attended lectures with Master's students in the analytical chemistry program. Previous studies provide much information regarding method development and were referenced and used in both projects. The literature also provided background information on the medical and industrial relevance of the topic from a biological perspective.

Researching the instruments and separation techniques referenced in the literature was indispensible as it facilitated understanding in the lab and I learned about various academic and industrial applications of analytical chemistry.

6. References

Banerjee, Shibdas, and Shyamalava Mazumdar. “Electrospray Ionization Mass Spectrometry: A Technique to Access the Information beyond the Molecular Weight of the Analyte.” *International Journal of Analytical Chemistry* 2012 (**2012**) 1–40.

Bodén , Niklas, and Lovisa Österlind. *Determination of 5-Hydroxyindoleacetic Acid in Urine Using High Performance Liquid Chromatography- Electrospray Ionization Tandem Mass Spectrometry* Department of Environmental Science and Analytical Chemistry, Stockholm University (**2019**)

Cohen, Steven A. *Quantitation of Amino Acids as 6-Aminoquinolyl-N-Hydroxysuccinimidyl Carbamate Derivatives J. of Chrom.* (**2005**) 242–267.

Cox, P. A., et al. *Biomagnification of Cyanobacterial Neurotoxins and Neurodegenerative Disease among the Chamorro People of Guam* Proc. of the Nat. Acad. of Sci. 100 (**2003**) 13380–13383.

Cox, P. A., et al. *Diverse Taxa of Cyanobacteria Produce -N-Methylamino-L-Alanine, a Neurotoxic Amino Acid* Proc. of the Nat. Ac. of Sci. 102 (**2005**) 5074–5078.

Denison, R. F., et al. *Reversible O2 Inhibition of Nitrogenase Activity in Attached Soybean Nodules* Plant Phys. 100 (**1992**) 1863–1868.

Downing, Simoné, and Timothy Grant Downing. *The Metabolism of the Non-Proteinogenic Amino Acid β-N-Methylamino-L-Alanine (BMAA) in the Cyanobacterium Synechocystis PCC6803* Toxicon 115 (**2016**) 41–48.

Downing, S., et al. *Nitrogen Starvation of Cyanobacteria Results in the Production of β-N-Methylamino-L-Alanine* Toxicon 58 (**2011**) 187–194.

Ferguson, Brett J., et al. *Molecular Analysis of Legume Nodule Development and Autoregulation* J. of Integr. Plant Bio. 52 (**2010**) 61–76.

Gonzalez, J. E., and M. M. Marketon. *Quorum Sensing in Nitrogen-Fixing Rhizobia*. Microbio. and Molec. Bio. Rev. 67 (**2003**) 574–592.

Gibson, Katherine E., et al. *Molecular Determinants of a Symbiotic Chronic Infection* Annual Rev. of Genetics 42 (**2008**) 413–441.

Grouzmann, Eric, et al. *Quantification of Vanillylmandelic Acid, Homovanillic Acid and 5-Hydroxyindoleacetic Acid in Urine Using a Dilute-and-Shoot and Ultra-High Pressure Liquid Chromatography Tandem Mass Spectrometry Method* Clin. Chem. and Lab. Med. 5 (**2018**) 1533–1541.

Herridge, David F., et al. *Global Inputs of Biological Nitrogen Fixation in Agricultural Systems* Plant and Soil, 311 (**2008**) 1–18.

Hoffman, Brian M., et al. *Mechanism of Nitrogen Fixation by Nitrogenase: The Next Stage* Chemical Reviews, 114 (**2014**) 4041–4062.

Janczarek, Monika, et al. *Signal Molecules and Cell-Surface Components Involved in Early Stages of the Legume–Rhizobium Interactions* Ap. Soil Ecol. 85 (**2015**) 94-113.

Kurland, L. K., and D. W. Mulder. *Epidemiologic Investigations of Amyotrophic Lateral Sclerosis: 1. Preliminary Report on Geographic Distribution, with Special Reference to the Mariana Islands, Including Clinical and Pathologic Observations* Neurology, 4 (**1954**) 355–355.

Lionetto, L., Lostia, A. M., Stigliano, A., Cardelli, P., & Simmaco, M. *HPLC–mass spectrometry method for quantitative detection of neuroendocrine tumor markers: Vanillylmandelic acid, homovanillic acid and 5-hydroxyindoleacetic acid*. Clinica Chimica Acta, 398(1), (**2008**). 53–56

Murch, S. J., et al. *Occurrence of Beta-Methylamino-l-Alanine (BMAA) in ALS/PDC Patients from Guam* Acta Neurologica Scandinavica, 110 (**2004**) 267–269.

Nunn, Peter B. *50 Years of Research on α-Amino-β-Methylaminopropionic Acid (β-Methylaminoalanine)* Phytochem. 144 (**2017**) 271–281.

Peters, John W, and Robert K Szilagyi. *Exploring New Frontiers of Nitrogenase Structure and Mechanism* Current Op. in Chem. Bio., 10 (**2006**) 101–108.

Spáčil, Zdeněk, et al. *Analytical Protocol for Identification of BMAA and DAB in Biological Samples* Analyst, 135 (**2010**) 127–132.

Spencer, Peter S. *Guam ALS/Parkinsonism-Dementia: A Long-Latency Neurotoxic Disorder Caused by 'Slow Toxin(s)' in Food? Can. J. of Neuro. Sci* 14, no. S3, (**1987**), 347–357.

Vance, C. P. *Symbiotic Nitrogen Fixation and Phosphorus Acquisition. Plant Nutrition in a World of Declining Renewable Resources* Plant Physiology, 127, no. 2, (**2001**) 390–397.

"Method and Technique Development for the Analytical Chain ACES." *https://www.aces.su.se/* Stockholm University, www.aces.su.se/research/topics/method-and-technique-development-for-the-analytical-chain/.

7. Appendix

Appendix 1: Tissue Extraction

Root nodules were flash-frozen with liquid nitrogen and ground with pre-chilled mortar. Ground nodules were transferred to a 1.5 ml Eppendorf tube, extracted with 2:2:1 methanol:chloroform:water and vortexted. Samples were also sonicated for 10 minutes at 20 kV, and then centrifuged at 15,000 x *g* for 15 min, and the aqueous supernatant was collected as well as the organic phase into two new eppendorfs. Cavitation @ >20kH used for cell lysis (breaks cell membranes apart to release their contents)

Excess plant material was discarded and both the organic and aqueous phases were then dried using $N_{2(g)}$ and stored at -20 ºC. The organic phase was later reconstituted using MeOH and the aqueous phase using HCl.

Appendix 2: BMAA

BMAA (β-methylamino-L-alanine) is a naturally occurring non-proteinogenic amino acid linked to neurodegenerative disease. BMAA becomes neurotoxic when the tRNA Serine misincorporates it during protein synthesis, causing proteins to misfold expose hydrophilic parts, causing aggregation.

After high rates of Parkinson's disease (PD) and amyotrophic lateral sclerosis (ALS) were observed in the Chamarro people of Guam, BMAA was isolated from *Cycas micronesia* seeds, a staple of the Chamarro diet [Kurland 1954; Vega and Bell 1967]. Clinical testing further suggested neurotoxicity and brain tissue of affected patients also contained significant concentrations of BMAA [Spencer 1986, 1987; Murch 2004]. Because BMAA is produced by almost all cyanobacteria and algae found in aqueous environments, the human diet likely contains high concentrations of BMAA due to bioaccumulation [Cox 2003, 2005].

The possibility that BMAA could be produced by nitrogen-fixing Cyanobacteria implicated in symbiosis within plants other than *Cycas Micronesia* has previously been examined. In 2003, Cox et al. found significant concentrations of BMAA were in non-coralloidal tissue samples from three taxonomically distinct plants. BMAA was also found to be produced by cyanobacteria during nitrogen starvation, though whether it performs a function or provides nitrogen remains inconclusive [Downing 2011]. Data from an *in vitro* study using Isotopically labeled BMAA *Synechocystis* PCC6803 suggested that BMAA is metabolized through transanimation with the enzyme GOGAT to produce L-glutamate from α-ketoglutarate [Downing 2016].

Appendix 3: Derivatization

Derivatization uses a specific reagent to chemically modify an analyte's polarity, increasing or decreasing its affinity for the stationary or mobile phase. In theory the chromatographic response from a derivatized compound will be distinguishable from peaks that would have otherwise had similar or identical elution times (i.e., isomers).

Figure 1a: Derivatization of amino acids with 6-aminoquinolyl-N-hydroxysuccinimidyl carbamate [Cohen 2005]

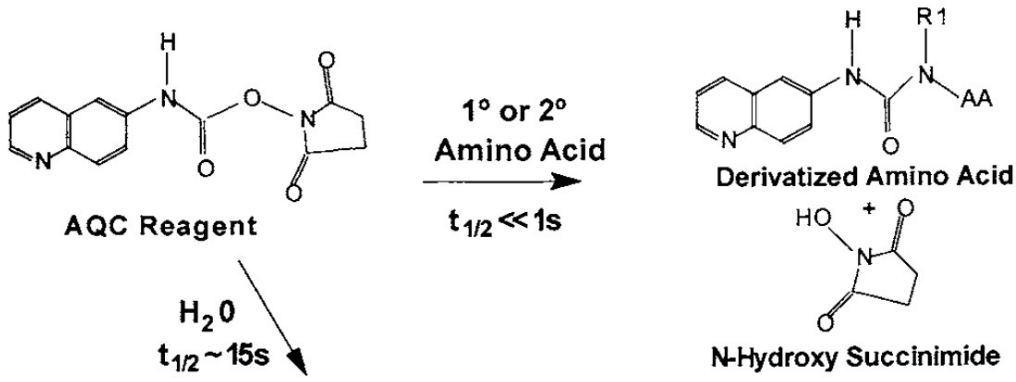

Figure 2a: Product Ion spectra for AQC derivatized BMAA and its isomer DAB. AQC-DAB and AQC-BMAA have the same parent mass of 459.1 m/z but different product ions (circled), allowing for tandem monitoring of two transitions [Spacil 2010].

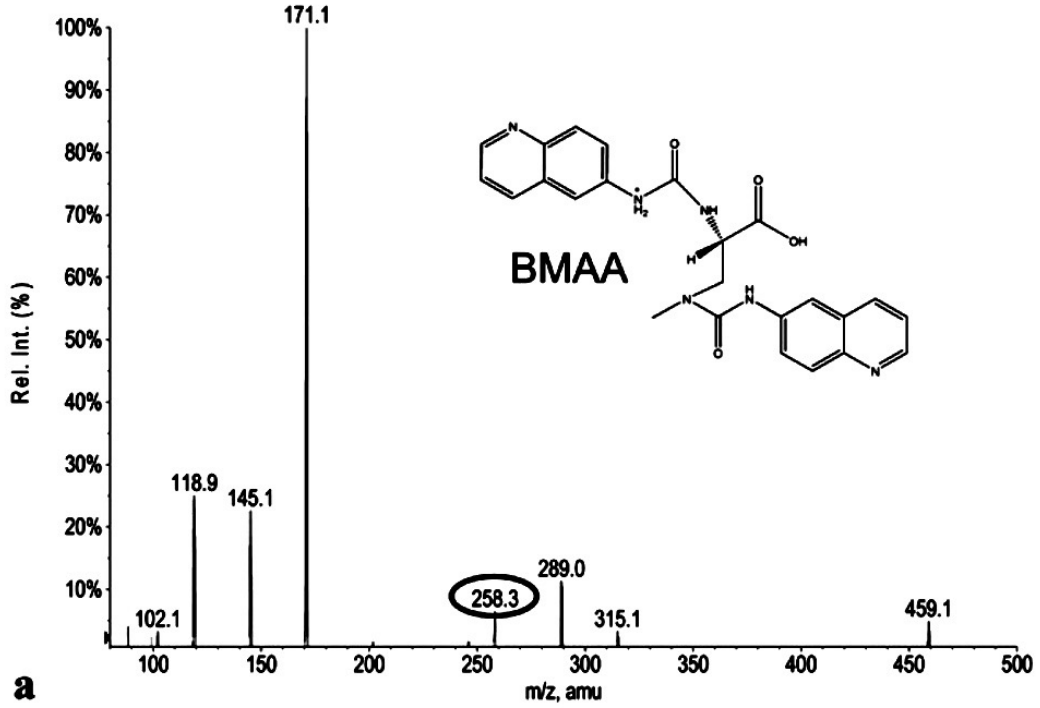

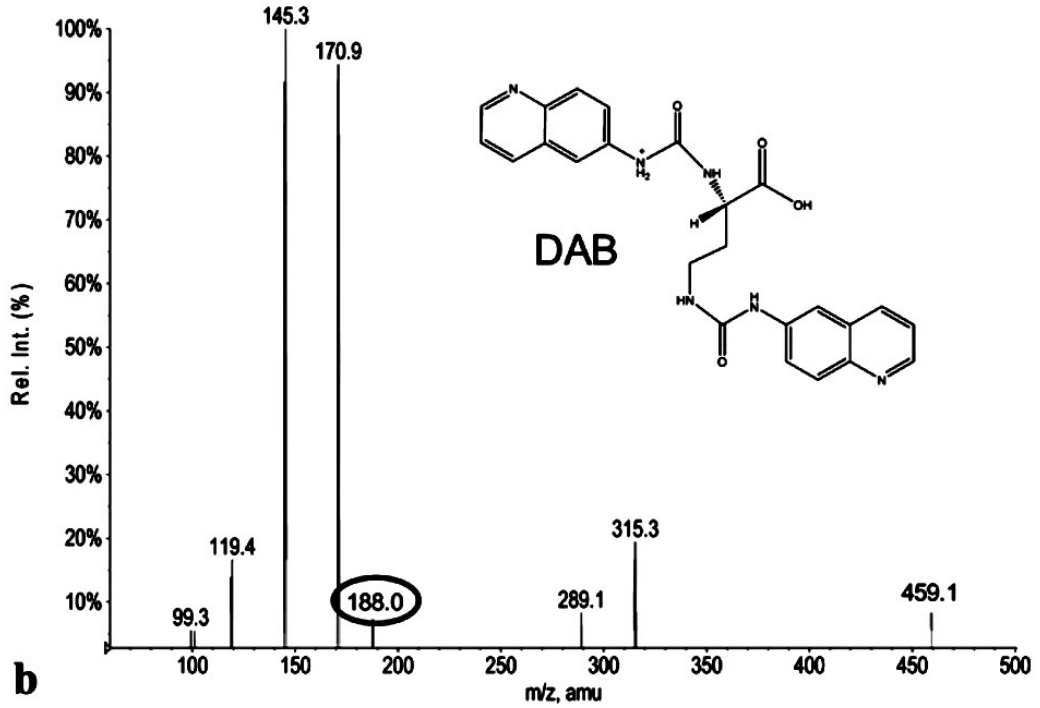

Appendix 4: Standard Preparation

Standard mass weighed = 2.5 mg. 10 µg/ml ,1 µg/ml, 1 ng/ml needed

CmVm = CfVf
Cm = concentration of original solution
Vm = Volume of starting solution to be pipetted
Cf = concentration of desired solution
Vf = volume of desired solution

10 µg solution: (Using 2.5 mg/ml solution)

$2.5 \cdot 10^3$ µg → 10^3 µL Vm = 10^3 µL • 10 µg / $2.5 \cdot 10^3$ µg
10 µg → Vm Vm = 4 µL

Figure 3a: Schematization of two-step dilution for Vm < 10 µL:

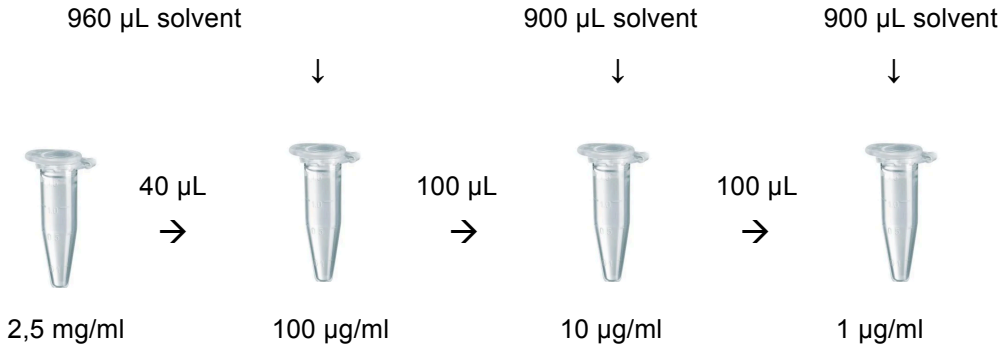

1 µg solution: (using 10 µg solution)

10 µg → 10^3 µL Vm = 10^3 µL • 1 µg / 10 µg
1 µg → Vm Vm = 100 µL

1 ng solution: (using 1 µg solution)

1 µg → 10^3 µL Vm = 10^3 µL • 10^{-3} µg / 1 µg
1 ng → Vm Vm = 1 µL

Deuterated or isotopically labeled ISs increase compound mass without affecting chemical properties so the IS's chromatographic behavior will be very similar to the analyte's. Mass distinction allows for parallel monitoring of distinct transitions producing specific response data sets (Area under peak after

integration). The IS is used as a reference for responses from analytes contained within samples for each run.